

# Optimized Intermolecular Potential Functions for Liquid Alcohols

William L. Jorgensen

Department of Chemistry, Purdue University, West Lafayette, Indiana 47907 (Received: September 24, 1985)

Intermolecular potential functions have been developed for use in computer simulations of liquid alcohols and other molecules with hydroxyl groups. The functions are based on earlier work for liquid hydrocarbons and required introduction of few new parameters. Optimization of the parameters involved studies of hydrogen-bonded complexes and Monte Carlo simulations for liquid methanol. Further application then consisted of Monte Carlo simulations for liquid methanol, ethanol, 1-propanol, 2-propanol, and 2-methyl-2-propanol at 25 °C and 1 atm. Extensive thermodynamic and structural results are reported for the liquid alcohols and are compared with experimental data. The excellent accord between simulation and experiment is remarkable in view of the simple form and facile parametrization of the potential functions. The five liquid alcohols all feature winding hydrogen-bonded chains with averages of close to two hydrogen bonds per molecule. The hydrogen bonding is also found to have interesting effects on the torsional energy surfaces for molecules in the liquids. Most striking is a narrowing of the conformational energy wells for rotation about the C-O bonds.

## Introduction

Computer simulations offer the opportunity of obtaining detailed insights into the structure and dynamics of molecular systems.<sup>1</sup> A key issue underlying the success of the computations is the need for potential functions that properly describe the interatomic interactions in the modeled systems. Though much effort has gone into the development of intramolecular force fields for peptides,<sup>2,3</sup> the basis for the parametrization of intermolecular interactions for organic and biochemical systems has been limited. A primary difficulty associated with the nonbonded terms is that they should properly be developed and tested through comparisons of experiment and simulations for condensed-phase systems. This is demanding of computer resources; however, it is the approach that we have been taking for the generation of a set of intermolecular potential functions suitable for computer simulations of organic fluids and proteins in their native environment.<sup>4-9</sup> The functions have been derived primarily by fitting directly to experimental thermodynamic and structural data on pure organic liquids, liquid water, and aqueous solutions of organic molecules and ions representative of peptide constituents. The specific systems treated so far include a series of pure liquid hydrocarbons,<sup>4</sup> liquid water,<sup>5</sup> liquid amides,<sup>6</sup> and aqueous solutions of hydrocarbons,<sup>7</sup> amides,<sup>8</sup> carboxylate ions,<sup>9</sup> and ammonium ions.<sup>9</sup>

In the present work, the treatment has been extended to liquid alcohols. This is a particularly important class of compounds due to their amphiphilic character, their importance as organic solvents, and the occurrence of hydroxyl groups in the side chains for serine, threonine, tyrosine, and several less common amino acids. The present study includes results from Monte Carlo statistical mechanics simulations for liquid methanol, ethanol, 1-propanol, 2-propanol, and 2-methyl-2-propanol, so all branching patterns are represented. Among these alcohols, methanol<sup>10-12</sup> and ethanol<sup>13</sup> have been the subjects of prior fluid simulations by our group, and only methanol has been modeled by another group.<sup>14</sup> In

TABLE I: Computational Details of the Monte Carlo Simulations of Liquid Alcohols at 25 °C

alcohol	no. of config × 10 <sup>-6</sup>		$r_c$ , Å	$\Delta r$ , Å	$\Delta\theta$ , deg	$\Delta\phi$ , deg	$\Delta V$ , Å <sup>3</sup>
	equil	averaging					
methanol	1.0	2.0	9.5	0.19	19		220
ethanol	2.2	2.0	11.0	0.15	15	15	250
1-propanol	0.9	2.0	11.5	0.14	10	15	400
2-propanol	1.8	2.0	11.5	0.14	14	15	400
2-methyl-2-propanol	1.6	3.0	12.0	0.14	14	15	400

contrast, the structure and hydrogen bonding in liquid alcohols have been investigated in numerous spectroscopic<sup>15</sup> and diffraction experiments.<sup>16-23</sup> The extensive structural information obtained from the simulations is shown below to be in good accord with the overall picture that has emerged from the experimental work. The computed thermodynamic results also agree closely with experimental data. In addition, some interesting condensed-phase effects are predicted for the conformational profiles of the liquid alcohols.

## Computational Details

**Monte Carlo Simulations.** The statistical mechanics calculations were carried out for the five liquid alcohols using standard procedures including Metropolis sampling, periodic boundary conditions, and the isothermal-isobaric (NPT) ensemble.<sup>4,6</sup> Each system consisted of 128 molecules in a cubic cell. The temperature and external pressure were fixed at 25 °C and 1 atm. This is well within the liquid region for these alcohols except for 2-methyl-2-propanol which melts at 25.5 °C at 1 atm.

Additional details are summarized in Table I. The intermolecular interactions were spherically truncated at cutoff distances,  $r_c$ , based on the O-O distance for methanol and C<sub>0</sub>-O<sub>0</sub> for the other systems. New configurations were generated by randomly selecting a monomer, translating it randomly in all three Cartesian directions, rotating it randomly about a randomly chosen axis, and performing any internal rotations (vide infra). The ranges

(1) For reviews, see: (a) McCammon, J. A. *Rep. Prog. Phys.* **1984**, *47*, 1. (b) Jorgensen, W. L. *J. Phys. Chem.* **1983**, *87*, 5304.

(2) For a review, see: Levitt, M. *Annu. Rev. Biophys. Bioeng.* **1982**, *11*, 251.

(3) Weiner, S. J.; Kollman, P. A.; Case, D. A.; Singh, U. C.; Ghio, C.; Alagona, G.; Profeta, S., Jr.; Weiner, P. *J. Am. Chem. Soc.* **1984**, *106*, 765.

(4) Jorgensen, W. L.; Madura, J. D.; Swenson, C. J. *J. Am. Chem. Soc.* **1984**, *106*, 6638.

(5) Jorgensen, W. L.; Chandrasekhar, J.; Madura, J. D.; Impey, R. W.; Klein, M. L. *J. Chem. Phys.* **1983**, *79*, 926. Jorgensen, W. L.; Madura, J. D. *Mol. Phys.* **1985**, *56*, 1381.

(6) Jorgensen, W. L.; Swenson, C. J. *J. Am. Chem. Soc.* **1985**, *107*, 569.

(7) Jorgensen, W. L.; Gao, J.; Ravimohan, C. *J. Phys. Chem.* **1985**, *89*, 3470.

(8) Jorgensen, W. L.; Swenson, C. J. *J. Am. Chem. Soc.* **1985**, *107*, 1489.

(9) Jorgensen, W. L.; Gao, J. *J. Phys. Chem.*, in press.

(10) Jorgensen, W. L. *J. Am. Chem. Soc.* **1980**, *102*, 543.

(11) Jorgensen, W. L. *J. Am. Chem. Soc.* **1981**, *103*, 341.

(12) Jorgensen, W. L.; Ibrahim, M. *J. Am. Chem. Soc.* **1982**, *104*, 373.

(13) Jorgensen, W. L. *J. Am. Chem. Soc.* **1981**, *103*, 345.

(14) Vij, J. K.; Reid, C. J.; Evans, M. W. *Mol. Phys.* **1983**, *50*, 935.

(15) For reviews, see: (a) Schuster, P.; Zundel, G.; Sandorfy, C., Eds. "The Hydrogen Bond"; North-Holland Publishing Co.: Amsterdam, 1976; Vol. 1-3. (b) Symons, M. C. R. *Chem. Soc. Rev.* **1983**, *12*, 1.

(16) Zachariasen, W. H. *J. Chem. Phys.* **1935**, *3*, 158.

(17) Harvey, G. G. *J. Chem. Phys.* **1938**, *6*, 111.

(18) Wertz, D. L.; Kruh, R. K. *J. Chem. Phys.* **1967**, *47*, 388.

(19) Magini, M.; Paschina, G.; Piccaluga, G. *J. Chem. Phys.* **1982**, *77*, 2051.

(20) Narten, A. H.; Habenschuss, A. *J. Chem. Phys.* **1984**, *80*, 3387.

(21) Montague, D. G.; Gibson, I. P.; Dore, J. C. *Mol. Phys.* **1981**, *44*, 1355; **1982**, *47*, 1405.

(22) Mikusinska-Planner, A. *Acta Crystallogr., Sect. A: Cryst. Phys., Diffraction, Theor. Gen. Crystallogr.* **1977**, *A33*, 433.

(23) Narten, A. H.; Sandler, S. I. *J. Chem. Phys.* **1979**, *71*, 2069.

TABLE II: Geometrical and OPLS Parameters for Alcohols

Standard Geometrical Parameters			
bond lengths, Å		bond angles, deg	
O-H	0.945	COH	108.5
C-O	1.430	CCO	108.0
C-C	1.530	CCC	112.0
OPLS Parameters			
atom or group	$q$	$\sigma$ , Å	$\epsilon$ , kcal/mol
O (COH)	-0.700	3.07	0.17
H (COH)	0.435	0.0	0.0
CH <sub>n</sub> (COH)	0.265	$\sigma(\text{CH}_n)^a$	$\epsilon(\text{CH}_n)^a$

<sup>a</sup>Standard alkyl group values from ref 4.

for the three types of motions are given by  $\pm\Delta r$ ,  $\pm\Delta\theta$ , and  $\pm\Delta\phi$  in Table I. Attempts to change the volume of the systems were made every 700 configurations within the ranges  $\pm\Delta V$ , and all intermolecular distances were scaled accordingly. The ranges were chosen to yield acceptance ratios of ca. 0.4 for new configurations.

Each simulation had an equilibration phase of  $(1-2) \times 10^6$  configurations which was discarded. Averaging for the computed properties then occurred over an additional  $2 \times 10^6$  configurations for all systems except 2-methyl-2-propanol. In the latter case,  $3 \times 10^6$  configurations were used to be certain that there was no drift in the thermodynamic results since the simulation is in the supercooled region. In fact, the energies and densities were all well converged within the equilibration periods. The starting configurations for methanol and ethanol were taken from the earlier studies.<sup>11-13</sup> Configurations of ethanol were transformed to the propyl alcohols, while 2-methyl-2-propanol was obtained from 2-propanol. Typically, these transformations involve increasing the volume and gradually growing in the new groups.

The statistical uncertainties ( $\pm 1\sigma$ ) reported here for the computed properties were obtained from separate averages over batches of  $2 \times 10^5$  configurations. These batches are large enough so that the accuracy of the uncertainties should be good except for the compressibilities.<sup>24</sup> The calculations were executed on the Gould 32/8750 computer in our laboratory.

**Intermolecular Potential Functions.** In expanding the set of optimized potentials for liquid simulations (OPLS) to cover alcohols, we have followed the same guidelines as in the earlier work.<sup>4-9</sup> Reasonable geometrical and energetic results are expected for gas-phase complexes; the computed densities and energies for the liquids should be within ca. 2% of the experimental values, and the simple Lennard-Jones plus Coulomb form for the potential functions should be maintained (eq 1). In eq 1,  $\Delta\epsilon_{ab}$  is the

$$\Delta\epsilon_{ab} = \sum_i \sum_j^{\text{on a on b}} (q_i q_j e^2 / r_{ij} + A_{ij} / r_{ij}^{12} - C_{ij} / r_{ij}^6) \quad (1)$$

interaction energy between molecules a and b, and standard combining rules are used such that  $A_{ij} = (A_{ii}A_{jj})^{1/2}$  and  $C_{ij} = (C_{ii}C_{jj})^{1/2}$ . The  $A$  and  $C$  parameters may also be expressed in terms of Lennard-Jones  $\sigma$ 's and  $\epsilon$ 's as  $A_{ii} = 4\epsilon_i\sigma_i^{12}$  and  $C_{ii} = 4\epsilon_i\sigma_i^6$ .

The molecules are represented as collections of interaction sites ( $i$  and  $j$  in eq 1). There is one site on each atom except for CH<sub>n</sub> groups which are taken as single units centered on carbon. Standard bond lengths and bond angles based on microwave structures are assumed as summarized in Table II.<sup>25</sup> These are kept fixed during the simulations, though torsional motion is included as discussed in the next section.

The parametrization for alcohols was initiated by studying hydrogen-bonded dimers and methanol-water complexes. The four-site TIP4P model for water was used in this context and is part of the OPLS set.<sup>5</sup> The Lennard-Jones parameters for the CH<sub>n</sub> groups were taken directly from the work on liquid hydrocarbons.<sup>4</sup> Prior experience with hydrogen-bonded systems in-

TABLE III: Fourier Coefficients for Intramolecular Rotational Potential Functions<sup>a</sup>

alcohol	bond	$V_0$	$V_1$	$V_2$	$V_3$
ethanol	C-O	0.0	0.834	-0.116	0.747
1-propanol	C-O	0.0	0.834	-0.116	0.747
	C1-C2	0.0	0.702	-0.212	3.060
2-propanol	C-O	0.429	0.784	0.125	-0.691
2-methyl-2-propanol	C-O	0.0	0.0	0.0	0.650

<sup>a</sup>Units for  $V$ 's are kcal/mol.

cluding alcohols suggested desirable patterns for charge distributions and the gas-phase complexes.<sup>5,6,11,13,26</sup> For example, the hydrogen bonds need to be ca. 0.2 Å shorter and 1 kcal/mol stronger than the best estimates for the gas phase. Charges are only placed on the atoms of the CH<sub>n</sub>-O-H units and need to yield dipole moments ca. 25% greater than for an isolated molecule.

The initial parameters derived in this way were then tested in a Monte Carlo simulation for liquid methanol. The density was a little low, so some adjustment seemed appropriate for the  $\sigma$  of oxygen. After this refinement, simulations were run for the five liquid alcohols. It was surprising to find that the same parameters could be used for the hydroxyl group with good success in each case. Remarkably, only four independent parameters had to be added to the OPLS set to describe alcohols, the charge,  $\epsilon$ , and  $\sigma$  for oxygen and the charge on hydrogen. The charge on C<sub>O</sub> is determined by neutrality, and the Lennard-Jones parameters for hydroxyl hydrogen are taken to be zero as before.<sup>5,6,26</sup> The  $\epsilon$  for oxygen was, in fact, simply assigned an average value based on oxygen in water and amides.<sup>5,6</sup> The parameters for alcohols are summarized in Table II. The charge assignments yield dipole moments of 2.2 D for the alcohols, a value similar to that for several models of water including TIP4P.<sup>5</sup> The  $\sigma$  for oxygen is also in a reasonable range about midway between the values in water (3.15 Å) and amides (2.96 Å).<sup>5,6</sup>

The parameters derived here for alcohols are similar to those in the original TIPS model.<sup>26</sup> Specifically, the TIPS values for  $\sigma$  and  $\epsilon$  of oxygen are 3.08 Å and 0.175 kcal/mol. However, the charge separation between oxygen (-0.685e) and hydrogen (0.40e) is somewhat less than with the new parameters. As described below, this results in a ca. 1 kcal/mol strengthening of hydrogen bonds with the new model and significantly improved energetic results for the liquid alcohols. The OPLS parameters for CH<sub>n</sub> groups also represent a significant improvement, particularly for branched systems.<sup>4</sup>

**Internal Rotation.** Torsional motion about the C-O bonds was included in the simulations for ethanol, 1-propanol, 2-propanol, and 2-methyl-2-propanol. A second dihedral angle was also needed for 1-propanol about the C1-C2 bond. A review on the implementation of the internal rotations in such calculations is available and can be consulted for details.<sup>1b</sup>

For the molecules with a single dihedral angle, the Fourier series in eq 2 suffices to describe the potential energy for internal ro-

$$V(\phi) = V_0 + \frac{1}{2}V_1(1 + \cos \phi) + \frac{1}{2}V_2(1 - \cos 2\phi) + \frac{1}{2}V_3(1 + \cos 3\phi) \quad (2)$$

tation. For 1-propanol, a separate Fourier series is used for each dihedral angle augmented by a Lennard-Jones term for the 1-5 interaction between H<sub>O</sub> and the methyl group.<sup>4</sup> As in the study of hydrocarbons,<sup>4</sup> the Fourier coefficients and Lennard-Jones parameters were determined by fitting to the rotational potentials obtained from MM2 molecular mechanics calculations with full geometry optimization.<sup>27</sup> The rotational potentials for ethanol, 2-propanol, and 2-methyl-2-propanol are shown in the top parts of Figures 1-3, and the Fourier coefficients are recorded in Table III. The Lennard-Jones parameters for the 1-5 interaction in 1-propanol are  $\sigma_{\text{CH}} = 2.6$  Å and  $\epsilon_{\text{CH}} = 0.008$  kcal/mol.

(24) Jorgensen, W. L. *Chem. Phys. Lett.* **1982**, *92*, 405.

(25) Harmony, M. D.; Laurie, V. W.; Kuczowski, R. L.; Schwendeman, R. H.; Ramsay, D. A.; Lovas, F. J.; Lafferty, W. J.; Maki, A. G. *J. Phys. Chem. Ref. Data* **1979**, *8*, 619.

(26) Jorgensen, W. L. *J. Am. Chem. Soc.* **1981**, *103*, 335.

(27) Allinger, N. L.; Chang, S. H.-M.; Glaser, D. H.; Honig, H. *Isr. J. Chem.* **1980**, *20*, 51.

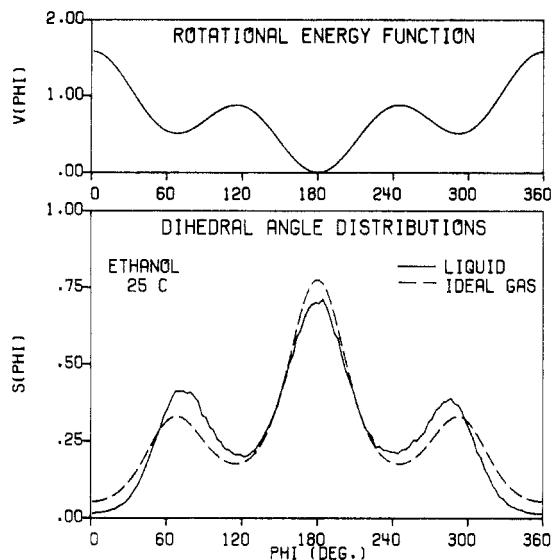


**Figure 1.** Rotational energy function and dihedral angle distributions for ethanol. Units are kcal/mol for  $V(\phi)$  and mole percent per degree for  $s(\phi)$  in Figures 1–5.

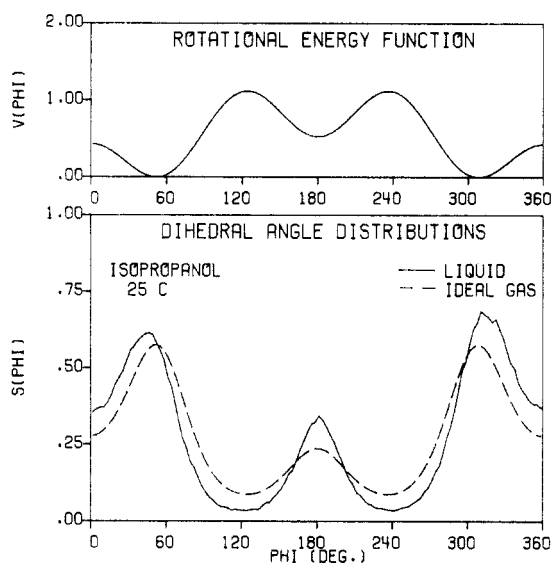


**Figure 2.** Rotational energy function and dihedral angle distributions for 2-propanol.

Ethanol has one trans and two mirror-image gauche conformers (Figure 1). The trans–gauche energy difference of 0.51 kcal/mol from the potential function agrees well with a recent value of  $0.7 \pm 0.1$  kcal/mol from overtone spectra.<sup>28</sup> It is also in accord with the results of ab initio calculations at the 4–31G level, 0.64 kcal/mol.<sup>29</sup> However, a lower estimate of  $0.12 \pm 0.01$  kcal/mol has been obtained from microwave spectroscopy.<sup>30</sup> The trans–gauche barrier and the cis maximum are at 0.88 and 1.58 kcal/mol in Figure 1. The corresponding 4–31G results are 1.35 and 2.06 kcal/mol.<sup>13,29</sup>

2-Propanol also has a trans form with the hydroxyl hydrogen between the two methyl groups and two mirror-image gauche forms (Figure 2). The trans conformer is now 0.52 kcal/mol higher in energy than the gauche rotamers according to the MM2 results. Experimental estimates of 0.6,  $0.45 \pm 0.21$ , <0.2, and 0.03 kcal/mol can be cited from IR,<sup>31</sup> microwave,<sup>32</sup> overtone,<sup>28</sup> and far-IR<sup>33</sup> analyses, respectively. The gauche–trans and

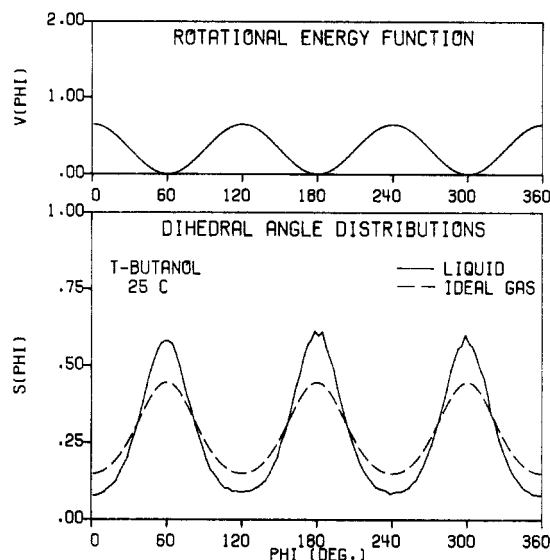


**Figure 3.** Rotational energy function and dihedral angle distributions for 2-methyl-2-propanol.

**TABLE IV: Calculated Hydrogen-Bond Energies and Geometries for Bimolecular Complexes**

complex <sup>a</sup>	$r_{OO}$ , Å	$\theta$ , deg	$-\Delta E$
HOH...OH <sub>2</sub>	2.75	46	6.24
cyclic (H <sub>2</sub> O) <sub>2</sub>	2.79	42	4.77
MeOH...OH <sub>2</sub>	2.77	42	6.03
HOH...OHMe	2.72	23	6.77
MeOH...OHMe	2.73	22	6.80
cyclic (MeOH) <sub>2</sub>	2.75	44	4.92
EtOH...OHEt	2.74	22	7.04
2-PrOH...OH-2-Pr	2.74	22	7.55
2-Me-2-PrOH...OH-2-Me-2-Pr	2.88	19	6.68

<sup>a</sup> Linear hydrogen-bonded complexes ( $\angle O-H...O \equiv 180^\circ$ ) except for the two cyclic dimers.

gauche–gauche barrier heights are 1.12 and 0.43 kcal/mol in Figure 2.

The torsional potential for 2-methyl-2-propanol has threefold symmetry with a calculated energy difference of 0.65 kcal/mol between the staggered and eclipsed rotamers (Figure 3). Experimental estimates for the barrier do not appear to be available. The reduction of the barrier from the microwave value of 1.07 kcal/mol for methanol does not seem unreasonable.<sup>34</sup>

For 1-propanol, a two-dimensional fit was made to the MM2 torsional results. It was found that the Fourier series for the first dihedral angle (C–O) was well described by the rotational potential for ethanol. The Fourier coefficients for the second angle were fit to the results with the first angle fixed in the trans form. The Lennard-Jones term was then needed to provide a little added repulsion near the doubly cis conformer. The following pairs of energies (in kcal/mol) compare the results from the potential function and MM2 calculations for key conformers, where t and g stand for trans and gauche: tt (0, 0), tg (0.36, 0.37), gt (0.54, 0.54), g<sup>+</sup>g<sup>+</sup> (0.90, 0.86), g<sup>+</sup>g<sup>−</sup> (0.92, 1.18), and cis–cis (6.94, 6.79). Only the last form is not a minimum. The experimental data for this system are limited, though the gt conformer has been estimated to be 0.4 kcal/mol above tt from overtone spectra.<sup>28</sup>

In the Monte Carlo simulations, an attempt was made to change the dihedral angle(s) for a monomer each time it was moved.<sup>1b</sup> To facilitate the conformational transitions, umbrella sampling was used for 1-propanol. The trans–gauche and gauche–gauche barriers for the C1–C2 dihedral angle were chopped at 2.4 and 3.0 kcal/mol, respectively.<sup>1b</sup> The torsional barriers are sufficiently low for the rotations about the C–O bonds that umbrella sampling was not needed in these cases. Conformational equilibrium was

(28) Fang, H. L.; Swofford, R. L. *Chem. Phys. Lett.* **1984**, *105*, 5.

(29) Radom, L.; Hehre, W. J.; Pople, J. A. *J. Am. Chem. Soc.* **1972**, *94*, 2371.

(30) Kakar, P. K.; Quade, C. R. *J. Chem. Phys.* **1980**, *72*, 4300.

(31) Kolbe, A. Z. *Phys. Chem. (Leipzig)* **1972**, *250*, S183.

(32) Hirota, E. *J. Phys. Chem.* **1979**, *83*, 1457.

(33) Inagaki, F.; Harada, I.; Shimanouchi, T. *J. Mol. Spectrosc.* **1973**, *46*, 381.

(34) Lees, R. M.; Baker, J. G. *J. Chem. Phys.* **1968**, *48*, 5299.

TABLE V: Energetic Results for Liquid Alcohols at 25 °C<sup>a</sup>

alcohol	$-E_i$	$E_{\text{intra}}(\text{g})$	$E_{\text{intra}}(\text{l})$	$H^\circ - H^b$	$\Delta H_{\text{vap}}$	
					calcd	exptl <sup>b</sup>
methanol	$8.59 \pm 0.02$	0.0	0.0	0.13	$9.05 \pm 0.02$	8.94
ethanol	$9.45 \pm 0.02$	0.496	$0.486 \pm 0.002$	0.06	$9.99 \pm 0.02$	10.11
1-propanol	$10.75 \pm 0.02$	1.025	$1.009 \pm 0.004$	0.02	$11.34 \pm 0.02$	11.36
2-propanol	$10.61 \pm 0.03$	0.328	$0.276 \pm 0.002$	0.01	$11.24 \pm 0.03$	10.85
2-methyl-2-propanol	$10.49 \pm 0.03$	0.239	$0.181 \pm 0.002$	0.05	$11.09 \pm 0.03$	11.14

<sup>a</sup> Energies in kcal/mol. <sup>b</sup> Reference 38.

readily established in each system as illustrated below.

## Results and Discussion

**Hydrogen-Bonded Complexes.** Geometry optimizations were carried out for hydrogen-bonded alcohol dimers and methanol-water complexes as summarized in Table IV. For the linear dimers, the O—O distance and the angle  $\theta$  between the hydrogen-bond vector and the bisector of the ROH angle of the hydrogen bond acceptor were optimized. The hydrogen-bond angle, O—H...O, was fixed at 180° in this case. The cyclic dimers were constrained to be planar, and  $\theta$  is the O...O—H angle in this instance. For ethanol and 2-propanol, the monomers are in the trans form, and the staggered geometry is used for 2-methyl-2-propanol.

The results provide an indication of optimal hydrogen-bonding energies and geometries for these systems. The hydrogen-bond lengths are nearly constant at 2.7–2.8 Å except for the slightly larger value for the 2-methyl-2-propanol dimer. The linear alcohol dimers are flatter (smaller  $\theta$ ) than the TIP4P water dimer, though the force constant for this angle is small. The difference results from the negative charge being offset from the oxygen in the TIP4P model; the SPC and TIP3P potentials for water have the negative charge on oxygen and yield  $\theta$  values of 26–27°. The hydrogen bonds for the linear dimers also become progressively stronger with increasing size from water to 2-propanol. The trend is clearly due to increased Lennard-Jones attraction for the larger systems, since the electrostatics are constant due to the invariant charge distribution for the alcohols. The reversal for 2-methyl-2-propanol dimer is readily explained by a steric clash between the hydrogen-bond donor and the nearest methyl group of the acceptor. This methyl group is absent in the trans conformers for ethanol and 2-propanol.

The best theoretical results for the series of water and methanol complexes are the ab initio 6-31G\* optimizations of Tse et al.<sup>35</sup> The hydrogen-bond lengths are uniformly about 0.2 Å longer, the angle  $\theta$  for the linear forms is 42° to 55°, and the hydrogen bonds are ca. 1 kcal/mol weaker than the results from the OPLS functions. The shorter and stronger hydrogen bonds are needed for the liquid simulations to make up for the lack of explicit three-body and higher order cooperative effects.<sup>5</sup> The order of hydrogen-bond strengths agrees well with the 6-31G\* results. In particular, water is predicted by both calculations to be a somewhat better hydrogen-bond donor than acceptor with methanol.

The results for one additional complex, Na<sup>+</sup>...OHCH<sub>3</sub>, are worth noting. By use of the parameters reported previously for Na<sup>+</sup>,<sup>36</sup> the optimal Na—O distance is 2.21 Å and the interaction energy is –26.2 kcal/mol. Best estimates of about 2.2 Å and –25 kcal/mol can be made for these quantities from ab initio results and experimental data.<sup>37</sup>

**Thermodynamics.** The thermodynamic results from the fluid simulations are compared with experimental data in Tables V–VII. The heat of vaporization is calculated from eq 3 and 4 where

$$\Delta E_{\text{vap}} = E_{\text{intra}}(\text{g}) - E_i(\text{l}) - E_{\text{intra}}(\text{l}) \quad (3)$$

$$\Delta H_{\text{vap}} = \Delta E_{\text{vap}} + RT - (H^\circ - H) \quad (4)$$

TABLE VI: Molecular Volumes and Densities for Liquid Alcohols at 25 °C

alcohol	$V, \text{\AA}^3$		$d, \text{g/cm}$	
	calcd	exptl <sup>a</sup>	calcd	exptl <sup>a</sup>
methanol	$70.1 \pm 0.3$	67.63	$0.759 \pm 0.003$	0.7866
ethanol	$102.3 \pm 0.3$	97.43	$0.748 \pm 0.003$	0.7851
1-propanol	$126.6 \pm 0.3$	124.76	$0.788 \pm 0.002$	0.7998
2-propanol	$128.1 \pm 0.3$	127.72	$0.779 \pm 0.002$	0.7813
2-methyl-2-propanol	$159.4 \pm 0.4$	157.54	$0.772 \pm 0.002$	0.7812

<sup>a</sup> Reference 38.TABLE VII: Heat Capacities and Isothermal Compressibilities for Liquid Alcohols at 25 °C<sup>a</sup>

alcohol	$C_p(\text{ig})^b$	$C_p(\text{l})$		$10^6 \kappa$	
		calcd	exptl <sup>b</sup>	calcd	exptl <sup>c</sup>
methanol	10.49	$20.0 \pm 1.1$	19.40	$108 \pm 12$	128
ethanol	15.64	$26.1 \pm 1.3$	26.76	$97 \pm 11$	116
1-propanol	20.82	$31.7 \pm 1.3$	33.7	$90 \pm 9$	104
2-propanol	21.21	$34.6 \pm 1.8$	36.06	$102 \pm 10$	116
2-methyl-2-propanol	27.10	$45.8 \pm 2.9$	52.61	$107 \pm 12$	

<sup>a</sup>  $C_p$  in cal/(mol deg);  $\kappa$  in atm<sup>–1</sup>. <sup>b</sup> Reference 38. <sup>c</sup> Reference 39.

$E_{\text{intra}}(\text{g})$  and  $E_{\text{intra}}(\text{l})$  are the intramolecular rotational energies for the gas and liquid,  $E_i(\text{l})$  is the intermolecular energy for the liquid, and  $H^\circ - H$  is the enthalpy departure function which gives the enthalpy difference between the real and ideal gas.  $E_{\text{intra}}(\text{g})$  is computed from a Boltzmann distribution for the torsional potential function, while the small  $H^\circ - H$  corrections are taken from experimental data.<sup>38</sup> It should be noted that  $E_i(\text{l})$  includes a correction for the Lennard-Jones interactions neglected beyond the cutoff distance,  $r_c$ . It amounts to ca. 2% of the total energy and was computed in a standard way, as described previously.<sup>4</sup> The heat capacity,  $C_p$ , for a liquid is estimated from the fluctuation in the intermolecular energy plus an intramolecular term taken as  $C_p$  for the ideal gas less  $R$ . The isothermal compressibility is calculated from the volume fluctuations and has a larger uncertainty than for the other computed quantities.<sup>40</sup> The coefficient of thermal expansion was also calculated from a fluctuation formula; however, it does not converge in simulations of the present length and is not reported. Finally, the average volume of the system is directly computed in NPT simulations and is readily translated into a molecular volume and density.

In Table V, the computed and experimental heats of vaporization are shown to be in excellent accord with an average difference of only 1.3%. The largest discrepancy, 3.6%, is for 2-propanol, though the relative heats of vaporization for the C<sub>3</sub>H<sub>7</sub>OH isomers are still in the correct order. The intramolecular energies in Table V are uniformly a little lower in the liquids than in the gas phase. This condensed-phase effect on the torsional profiles is analyzed in the next section. Turning to Table VI, it is demonstrated that the OPLS functions also yield excellent densities for liquid alcohols. The average deviation from the experimental values is 1.8%. The computed densities are uniformly a little low. The results for the heat capacities and compressibilities in Table

(35) Tse, Y. C.; Newton, M. D.; Allen, L. C. *Chem. Phys. Lett.* **1980**, *75*, 350.(36) Chandrasekhar, J.; Spellmeyer, D. C.; Jorgensen, W. L. *J. Am. Chem. Soc.* **1984**, *106*, 903.(37) Smith, S. F.; Chandrasekhar, J.; Jorgensen, W. L. *J. Phys. Chem.* **1982**, *86*, 3308.(38) Wilhoit, R. C.; Zwolinski, B. J. *J. Phys. Chem. Ref. Data, Suppl.* **1973**, *2*.(39) Sahli, B. P.; Gager, H.; Richard, A. J. *J. Chem. Thermodyn.* **1976**, *8*, 179.(40) Jorgensen, W. L. *Chem. Phys. Lett.* **1982**, *92*, 405.

TABLE VIII: Calculated Conformer Populations at 25 °C<sup>a</sup>

alcohol	conformer	% gas	% liquid
ethanol	t	52.3	50.7 ± 0.3
	g	47.7	49.3 ± 0.3
1-propanol	t <sub>1</sub>	52.7	50.3 ± 0.6
	g <sub>1</sub>	47.3	49.7 ± 0.6
	t <sub>2</sub>	47.9	54.2 ± 1.0
	g <sub>2</sub>	52.1	45.8 ± 1.0
2-propanol	t	18.0	16.8 ± 0.8
	g	82.0	83.2 ± 0.8

<sup>a</sup>t<sub>1</sub> and t<sub>2</sub> refer to the trans populations for rotation about the CO and C1C2 bonds. g<sub>1</sub> and g<sub>2</sub> are the corresponding gauche populations.

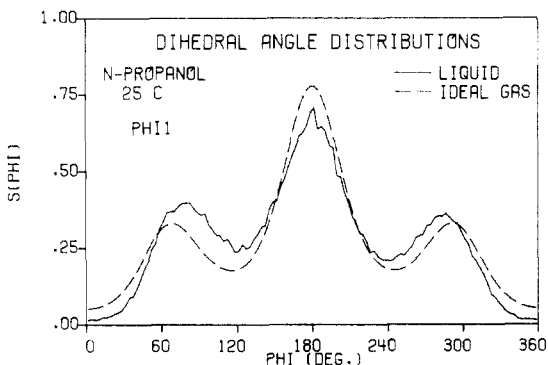


Figure 4. Dihedral angle distributions about the CO bond in 1-propanol.

VII are also in fine agreement with experimental data. It should be noted that the statistical uncertainties for the computed quantities are greater in these cases, and the ideal gas heat capacities less  $R$  make a substantial contribution to the total  $C_p$ . Overall, the thermodynamic results are impressive, particularly in view of the simple interaction model and trivial additional parametrization for the alcohols. Substantial improvement is apparent over the original TIPS results for methanol and ethanol which yielded errors of 10–15% for the densities and  $\Delta H_{vap}$ .<sup>11–13,41</sup>

**Conformational Equilibria.** The computed trans and gauche populations for the dihedral angles in liquid ethanol, 1-propanol, and 2-propanol are compared with the gas-phase values from Boltzmann distributions in Table VIII. Small condensed-phase effects are apparent. For rotation about the C–O bond in ethanol and 1-propanol, there is a ca. 2% increase in the gauche populations for the liquids. Energetically this is a small effect and should be interpreted cautiously. The implication is that there is probably a small steric preference for hydrogen bonding with a gauche molecule. It may be noted that the “lone-pair” region on oxygen is less encumbered by the alkyl chain, though the hydroxyl hydrogen is more encumbered, for the gauche rather than trans conformer. The conformational shift for the second dihedral angle in 1-propanol is greater with a 6.3% increase in the trans orientation. The gauche conformation around the C1–C2 bond clearly encumbers hydrogen bonding for 1-propanol irrespective of the conformation about the C–O bond. For 2-propanol, the 1.2% increase in the gauche population for the liquid is barely statistically significant. The hydroxyl hydrogen is more encumbered in the trans form, though part of the “lone-pair” region is more encumbered for gauche.

A particularly interesting effect is found for the full dihedral angle distributions in Figures 1–4. For rotation about the C–O bonds in ethanol, 1-propanol, 2-propanol, and 2-methyl-2-propanol, a significant narrowing of the conformational wells is apparent for the liquids vs. the gas phase. The effect is particularly striking for liquid 2-methyl-2-propanol (Figure 3) which shows enhanced preference for perfectly staggered geometries at dihedral angles of 60°, 180°, and 300°. This phenomenon is readily attributed to minimization of steric hindrance to hydrogen bonding. It also implies that the barriers for internal rotation are not the same in the gas and liquid; for 2-methyl-2-propanol, they are higher

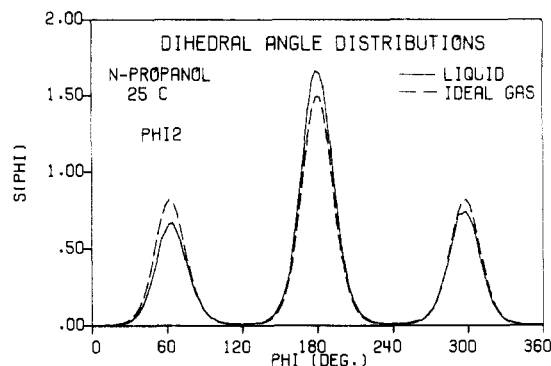


Figure 5. Dihedral angle distributions about the C1C2 bond in 1-propanol.

by about 0.5 kcal/mol in the liquid. For the C–O dihedral angles of ethanol and 1-propanol, the narrowing focuses on reducing the percentage of molecules in the liquids with nearly cis conformation. It also results in a shift of the gauche maxima in  $s(\phi)$  by a few degrees toward trans; i.e., the average dihedral angle for gauche molecules is a little different in the liquid and gas phases. For 2-propanol (Figure 2), significant narrowing of  $s(\phi)$  occurs for the trans conformer in the liquid. The shifts in the peak positions for the gauche rotamers are again understandable, since a shift toward 0° in this case puts the hydroxyl hydrogen farther from the nearest methyl group.

In contrast, the results for the dihedral angle about the C1–C2 bond in 1-propanol (Figure 5) do not show this behavior, nor is it found for liquid alkanes.<sup>4</sup> The increase in the trans population for the liquid is apparent in Figure 5 and was explained above. The lack of narrowing for the trans peak is reasonable since the methyl group is remote from the hydroxyl group in this form. Some narrowing could be expected for the gauche peaks to avoid cis more in the liquid. However, the gauche peaks are much narrower to begin with for this dihedral angle reflecting a deeper, narrower gauche well on the rotational energy surface than for rotation about the C–O bonds. Consequently, deformation is not as necessary and is more costly energetically in this case.

A few other points should be noted about the dihedral angle distributions in Figures 1–5. First, the thoroughness and uniformity of the sampling for the dihedral angles in the Monte Carlo simulations are apparent in the good symmetry obtained for each figure. Though some simulations were started far from equilibrium, the dihedral angle distributions and intramolecular energies were well converged within the equilibration segments. Also, the narrowing of the conformational wells discussed above is a key factor in the small reduction for  $E_{intra}(l)$  vs.  $E_{intra}(g)$  in Table V. The increased gauche populations for rotation about the C–O bonds in liquid ethanol and 1-propanol work against this trend. And, a technical point is that the  $s(\phi)$ 's for 1-propanol in the gas phase (Figures 4 and 5) are obtained by integrating over all values of the other dihedral angle.

The only earlier theoretical study that bears on these conformational issues was for liquid ethanol with the TIPS potentials.<sup>13</sup> Though the Monte Carlo simulation was only one-third the length of the present calculation, a  $2 \pm 1\%$  increase in the gauche population for the liquid was predicted.<sup>13</sup> Some narrowing of  $s(\phi)$  in the gauche regions is also apparent in the prior results. It was not noted, and it is not as pronounced due probably to the weaker hydrogen bonding with the TIPS functions. These conformational effects are undoubtedly sensitive to the details of the potential functions, particularly, the charge distributions.<sup>1b</sup> The choice of keeping the  $\beta$  carbons neutral for alcohols was supported previously by ab initio results.<sup>1b</sup> Results from alternative potential functions would be interesting as long as it is demonstrated that the potential functions provide thermodynamic results of comparable quality as those reported here.

**Radial Distribution Functions.** The computed atom–atom radial distribution functions (rdfs) between the COH units of the liquid alcohols are compared in Figures 6–11. The remaining rdfs are relatively less structured and are not presented here. Rdfs

(41) Jorgensen, W. L., unpublished results.

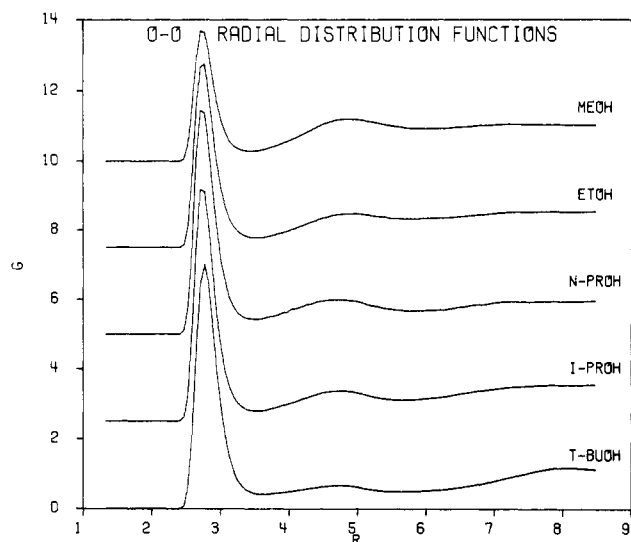


Figure 6. OO radial distribution functions for liquid alcohols. Distances in angstroms throughout. Successive curves offset 2.5 units along the y axis.

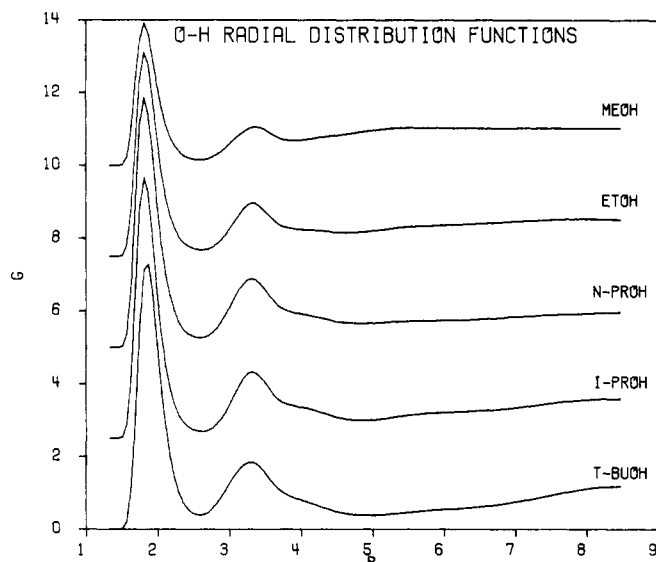


Figure 7. OH radial distribution functions for liquid alcohols. Successive curves offset 2.5 units along the y axis.

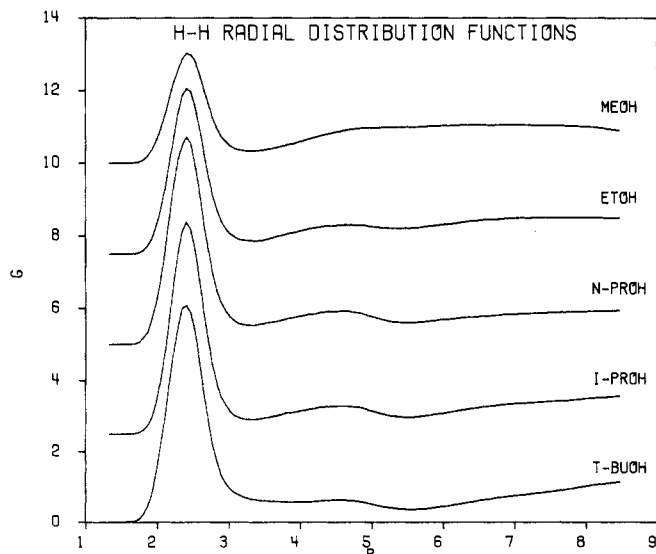


Figure 8. HH radial distribution functions for liquid alcohols. Successive curves offset 2.5 units along the y axis.

involving C2 in ethanol were reported previously.<sup>13</sup> In addition, extensive discussion of the rdfs for liquid methanol and ethanol

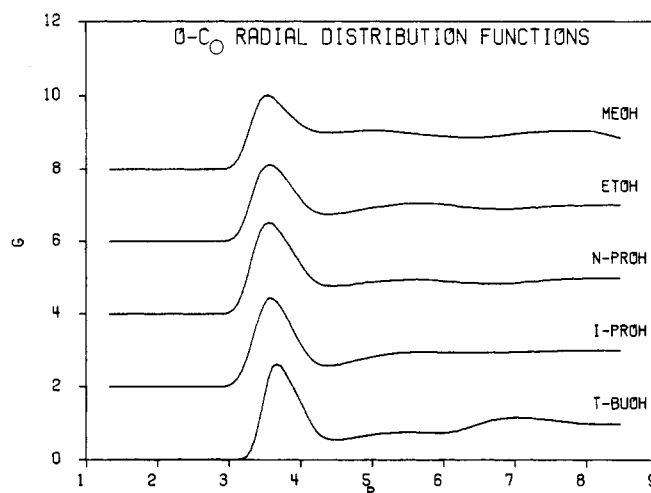


Figure 9. OC radial distribution functions for liquid alcohols. Successive curves offset 2 units along the y axis.

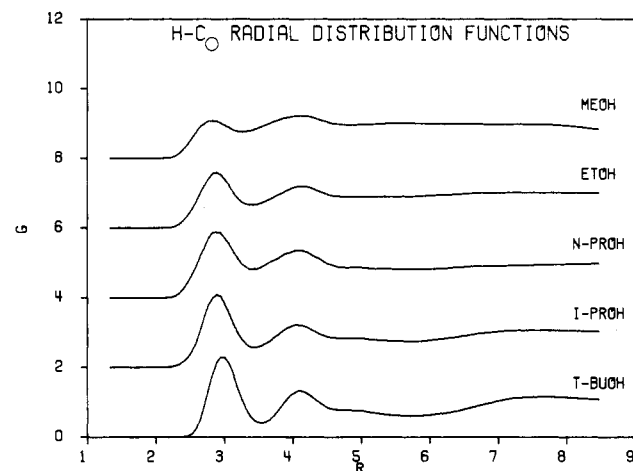


Figure 10. HO radial distribution functions for liquid alcohols. Successive curves offset 2 units along the y axis.

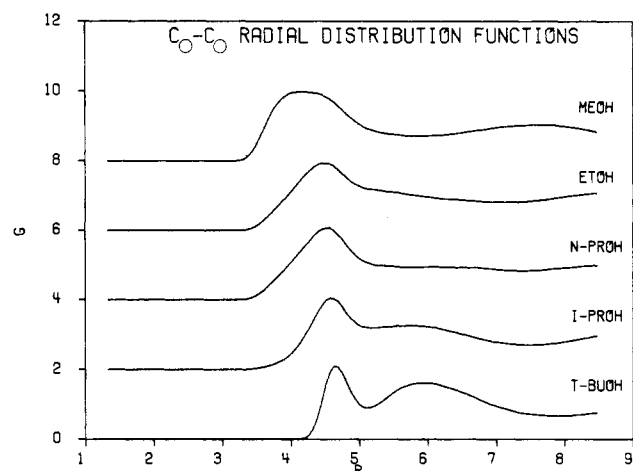
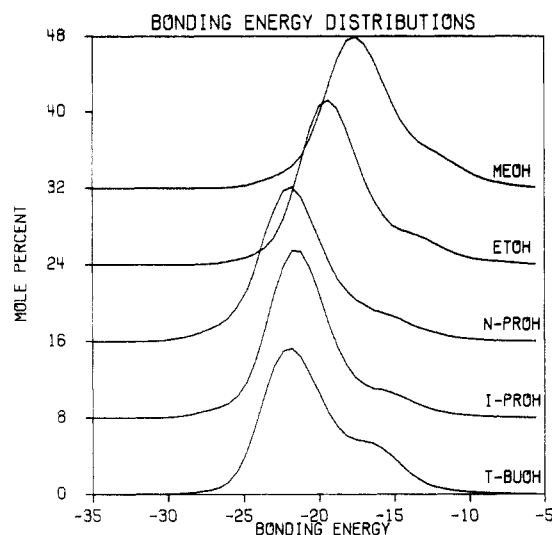


Figure 11. CO radial distribution functions for liquid alcohols. Successive curves offset 2 units along the y axis.

has already been presented.<sup>10-13</sup> Due to the similarities with the present results, the discussion will now be more condensed.

The sharp first peaks in the OO, OH, and HH rdfs (Figures 6-8) reflect the hydrogen bonding. The locations of the maxima of the first two peaks in the OO and OH rdfs are nearly invariant at 2.75 and 4.70 Å for OO and 1.82 and 3.30 Å for OH with uncertainties of ca.  $\pm 0.02$  Å. The integrals of the first peak in the OO rdfs to the minima at 3.4 Å are within 0.06 of 2.0 for each alcohol except 2-methyl-2-propanol which is 1.8 at 3.4 Å and reaches 2.0 at 3.85 Å. The first peaks in the OH rdfs out to 2.6 Å integrate to within 0.02 of 0.97 in all cases except 2-methyl-



**Figure 12.** Distributions of total intermolecular bonding energies for liquid alcohols. Bonding energies in kcal/mol. Units for the ordinate are mole percent per kcal/mol. Successive curves offset 8 units along the y axis.

2-propanol, 0.89. For the HH rdfs, the first peak locations are all at 2.35–2.40 Å and the integrals to 3.25 Å are all 2.1–2.2 except 1.95 for 2-methyl-2-propanol. These figures are clearly consistent with each molecule participating in an average two hydrogen bonds, one as donor and one as acceptor with slightly diminished hydrogen bonding for 2-methyl-2-propanol. As observed in the solids and previously for liquid methanol and ethanol, the dominant structural feature for all these liquids is winding hydrogen-bonded chains.<sup>10–13</sup> This is apparent in stereoplots of configurations and from the hydrogen-bonding analyses presented below.

The results on the location and area for the first peak in the OO rdf are in excellent agreement with X-ray diffraction data. For liquid methanol and ethanol, the peak has been reported at either 2.7 or 2.8 Å in recent studies<sup>18–20</sup> and between 2.6 and 2.9 Å including the older work.<sup>16,17</sup> The area of the peak has been found to be about 2,<sup>16–18</sup>  $1.8 \pm 0.1$ ,<sup>20</sup> and about 1.5.<sup>19</sup> The last value appears unlikely in view of the similarity of the theoretical and other experimental findings. X-ray results have also been reported for liquid 1-propanol at –25 °C and are consistent with a chain structure featuring a coordination number of 2 and 2.65 Å for the OO distance.<sup>22</sup> And, for liquid 2-methyl-2-propanol at 26 °C, Narten and Sandler found an OO separation of 2.74 Å and a coordination number of 2.<sup>23</sup>

The above data represent the key information derived from the diffraction experiments. The individual atom–atom rdfs have not yet been separated from the total  $g(r)$ . Due to numerous overlapping contributions from different atom pairs beyond 3.5 Å, the OO band is the principal one that stands out in the total radial distribution functions. Thus, there is also no experimental guidance on the peak heights in the rdfs. The increased peak heights in progressing from methanol to 2-methyl-2-propanol, seen particularly in Figures 6–8, result from the facts that the hydrogen bonding is relatively constant, but the number density of hydroxyl groups decreases with increasing molecular volume. In view of comparisons of experimental data and simulation results for liquid water, it would not be surprising if the heights of the first peaks in the present rdfs are overestimated by ca. 30%.<sup>5</sup> The origin of the discrepancy appears to be the lack of explicit three-body effects in the potential functions used in the theoretical work.<sup>5</sup>

Figures 9–11 contain the  $OC_O$ ,  $HC_O$ , and  $C_O C_O$  rdfs, respectively. The first peak in the  $OC_O$  rdf is due to the nearest neighbors and integrates to about two in each case. The  $HC_O$  rdf has two peaks since the hydroxyl hydrogen is nearer the hydrogen bond accepting neighbor than the donor. The first peak integrates to about one, as expected. The first peak in the  $C_O C_O$  rdf for methanol contains both intrachain and interchain contributions. The former are actually at larger separation as clarified by the progression to 2-methyl-2-propanol in Figure 11. Indeed, for

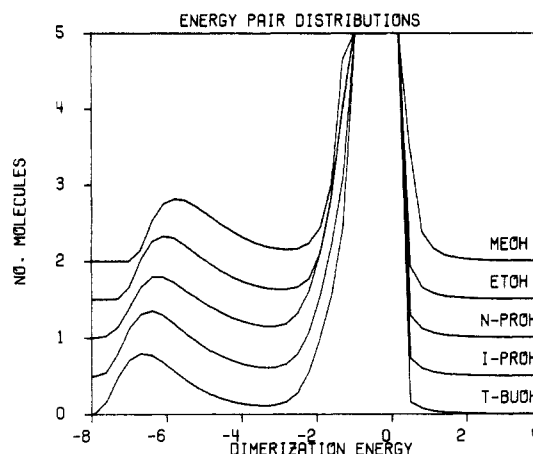


**Figure 13.** Distributions of individual interaction energies between molecules in liquid alcohols. Energies in kcal/mol. Units for the ordinate are number of molecules per kcal/mol. Successive curves are offset 0.5 unit along the y axis.

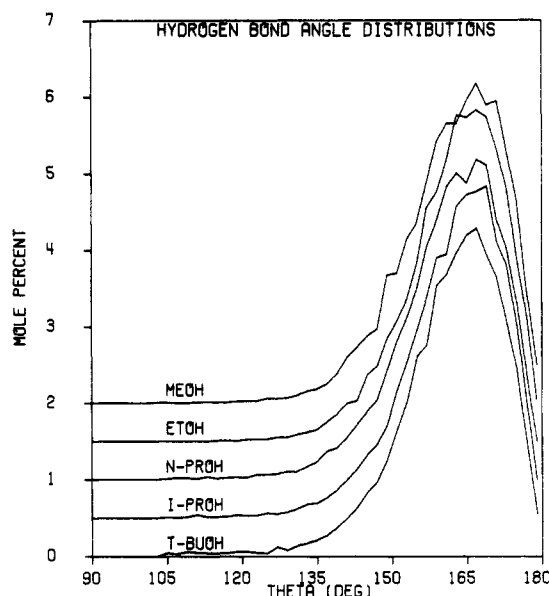


**Figure 14.** Distributions for the O–H...O hydrogen bond angle in liquid alcohols. Units for the ordinate are mole percent per degree. Successive curves offset 0.5 unit along the y axis.

2-methyl-2-propanol, the first peak in the  $C_O C_O$  rdf does integrate to about two.

**Energy Distributions.** The distributions in Figures 12 and 13 provide insight into the energetic environment in the liquids. Figure 12 contains the distributions of total intermolecular bonding energies for molecules in the liquids, while the distributions of individual molecule–molecule interactions are shown in Figure 13. From Figure 12 it is apparent that the molecules experience a range of energetic environments covering 20–25 kcal/mol. The profiles are bimodal as was found and fully analyzed in the earliest simulation of liquid methanol.<sup>10</sup> The band at higher energy reflects the molecules in zero or one hydrogen bond, while the larger band is due to the molecules in multiple hydrogen bonds. The separation is most pronounced for 2-methyl-2-propanol because the hydrogen-bond strengths are greater for the larger alcohols, so the gap between being in one or two hydrogen bonds is larger. Furthermore, 2-methyl-2-propanol has a larger percentage of molecules in zero or one hydrogen bond than the propanols (vide infra). It should also be noted that the curves in Figure 12 shift to lower energy with increasing size since they must parallel the trends in heats of vaporization.

The energy pair distributions in Figure 13 have the classic bimodal form for hydrogen-bonded liquids. The band at low energy corresponds to the hydrogen-bonded neighbors, while the spike from –2 to +0.5 kcal/mol reflects the numerous interactions

TABLE IX: Results of Hydrogen-Bond Analyses for Liquid Alcohols at 25 °C<sup>a</sup>

	methanol	ethanol	1-propanol	2-propanol	2-methyl-2-propanol
no. of H bonds	1.84	1.85	1.91	1.92	1.82
$\epsilon$ (H bond)	-5.19	-5.50	-5.66	-5.85	-6.04
$\epsilon$ (Coulomb)	-6.02	-6.01	-5.95	-5.98	-5.67
$\epsilon$ (LJ)	0.83	0.51	0.29	0.13	-0.37
$\theta$ , deg	162	162	161	162	162
$\phi$ , deg	119	118	116	117	115
% monomers in $n$ H bonds					
$n$	methanol	ethanol	1-propanol	2-propanol	2-methyl-2-propanol
0	1.8	2.2	1.1	0.9	1.2
1	19.0	14.7	14.2	11.9	18.3
2	72.9	78.6	77.0	82.0	77.7
3	6.2	4.4	7.6	5.6	2.6
4	0.0	0.0	0.1	0.0	0.1

<sup>a</sup>  $\epsilon$ 's in kcal/mol.  $\epsilon$ (H bond) is the average hydrogen-bond energy which can be decomposed into Coulomb,  $\epsilon$ (Coulomb), and Lennard-Jones,  $\epsilon$ (LJ), terms. A hydrogen bond is defined by an interaction energy of -3.0 kcal/mol or less.

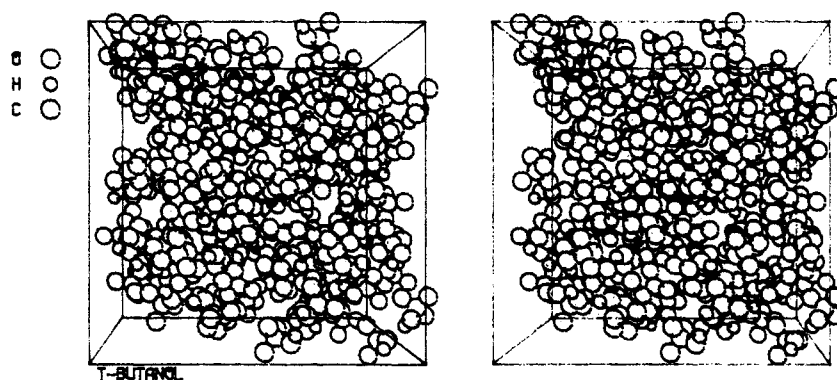


Figure 15. Stereoplot of a configuration from the Monte Carlo simulation of liquid 2-methyl-2-propanol.

with more distant molecules in the liquids. The low-energy bands can be integrated to obtain an estimate of the average number of hydrogen bonds per molecule. The result is sensitive to the integration limit; however, integrating to the minima near -3.0 kcal/mol yields 1.82–1.92 hydrogen bonds in each case as summarized in Table IX and discussed below.

**Hydrogen-Bonding Analyses.** The hydrogen bonding in the liquid alcohols was analyzed by using configurations saved every  $10^4$  steps during the Monte Carlo simulations. A hydrogen bond was defined by the energetic criterion of -3.0 kcal/mol suggested by the location of the minima in the energy pair distributions. The results for the average numbers of hydrogen bonds, hydrogen-bond energies, and hydrogen-bond angles are shown in Table IX.

The average number of hydrogen bonds is quite constant. The lower values for methanol (1.84) and ethanol (1.85) are attributable to use of the same energetic criterion in each case. Since the average hydrogen bond is weaker for these alcohols, a slightly higher cutoff might be appropriate. The hydrogen-bond strengths for 2-propanol and 2-methyl-2-propanol are similar; comparison then shows that 2-methyl-2-propanol does have about 5% fewer hydrogen bonds.

The breakdown into percentages of molecules in  $n$  hydrogen bonds is given in the bottom part of Table IX. The chain structure is consistent with the dominance of molecules in two hydrogen bonds. However, 3–8% of the monomers are in three hydrogen bonds, so there is some branching of the chains. There is also a significant percentage (12–19%) of chain ends, i.e., molecules in only one hydrogen bond. In addition, the calculations indicate the presence of 1–2% of monomer. Of course, the latter may have multiple interactions just above the cutoff which could still give them substantial total interaction energies, ca. 10–15 kcal/mol based on Figure 12. These notions are basically consistent with the interpretations in numerous studies of vibrational spectra in view of the variability of definitions of hydrogen bonds.<sup>15,42</sup> There

is little support for any free monomer, though the presence of small percentages of chain ends is confirmed. Consistent with the diffraction data, the present group of alcohols is not sufficiently hindered to cause departure from the average of about two hydrogen bonds per molecule. However, the presence of small oligomers can be substantial for more highly branched systems such as 2,6-diisopropylphenol.<sup>43,44</sup>

The data in Table IX also show the average hydrogen-bond energy declines from -5.2 kcal/mol for methanol to -6.0 kcal/mol for 2-methyl-2-propanol. The Coulombic contribution actually becomes less attractive along the series, but this is more than offset by the Lennard-Jones interactions becoming more favorable.

The average hydrogen-bond angles  $\theta$  (O-H...O) and  $\phi$  (H...O-H) are nearly invariant at about 162° and 117° for the alcohols. The full distributions for  $\theta$  are shown in Figure 14 and confirm the similarity over the entire angular range. These profiles are also similar to distributions obtained for O-H...O hydrogen bonds from analyses of numerous crystal structures.<sup>45,46</sup> The average hydrogen bond is bent about 20° from linearity; though from the results in many of the figures and Table IX, it is clear that a broad range of geometries and energies for hydrogen bonds is present in liquid alcohols.

In closing, a stereoplot of the last configuration from the simulation of liquid 2-methyl-2-propanol is shown in Figure 15. The edges of the box are a little outside the edges of the periodic cube. In viewing the plot, the periodicity should be recalled so molecules near one face are also interacting with molecules near the opposite face. The hydrogen bonding is evident with many molecules in two hydrogen bonds. Numerous winding chains are present, though the chain lengths are mostly unclear. There also appear to be some small oligomers including a possible cyclic tetramer

(43) Sendorfy, C. In ref 15a, Chapter 13.

(44) Jakobsen, R. J.; Mikawa, Y.; Brasch, J. W. *Appl. Spectrosc.* **1970**, *24*, 333.

(45) Olovsson, I.; Jonsson, P.-G. In ref 15a, Chapter 8.

(46) Kroon, J.; Kanters, J. A.; van Duijneveldt-van de Rijdt, J. G. C. M.; van Duijneveldt, F. B.; Vliegthart, J. A. *J. Mol. Struct.* **1975**, *24*, 109.

(42) Luck, W. A. P. In ref 15a, Chapters 11, 28. Luck, W. A. P.; Ditter, W. *Ber. Bunsenges. Phys. Chem.* **1968**, *72*, 365.

near the front of the cube in the lower left. Though the hydrogen bonding provides local structure, the overall picture reveals substantial disorder in comparison with crystal structures.

**Conclusion.** Intermolecular potential functions have been developed for use in computer simulations of alcohols. The success of the potential functions in yielding correct thermodynamic and structural descriptions of liquid alcohols is impressive in view of the simple form of the functions and the limited parametrization that was required. The structures of the five liquid alcohols studied here all feature winding hydrogen-bonded chains with averages of close to two hydrogen bonds per molecule. The hydrogen

bonding was found to have interesting effects on the torsional profiles for the liquids. There is a narrowing of the conformational potential energy wells for rotation about the C-O bonds which reduces steric hindrance to hydrogen bonding.

**Acknowledgment.** Gratitude is expressed to the National Science Foundation and National Institutes of Health for support of this research. The author is also grateful to James F. Blake and Jeffry D. Madura for assistance with plotting programs.

**Registry No.** MeOH, 67-56-1; EtOH, 64-17-5; CH<sub>3</sub>(CH<sub>2</sub>)<sub>2</sub>OH, 71-23-8; CH<sub>3</sub>CH(OH)CH<sub>3</sub>, 67-63-0; CH<sub>3</sub>C(CH<sub>3</sub>)(OH)CH<sub>3</sub>, 75-65-0.

## LASER CHEMISTRY, MOLECULAR DYNAMICS, AND ENERGY TRANSFER

### Effect of Variation in the Microenvironment of the Fractal Structure on the Donor Decay Curve Resulting from a One-Step Dipolar Energy-Transfer Process

C. L. Yang,<sup>†</sup> P. Evesque,<sup>‡</sup> and M. A. El-Sayed\*

Department of Chemistry and Biochemistry, University of California at Los Angeles, Los Angeles, California 90024 (Received: July 29, 1985; In Final Form: October 28, 1985)

A calculation is performed to determine the temporal behavior of the donor intensity,  $I(t)$ , via a one-step dipolar energy-transfer process on a structure of Euclidean dimension  $d = 2$  and a fractal dimension,  $D$ , ranging from 1.75 to 1.0. The results are fitted to the Klafter and Blumen equation, useful in analyzing experimental data to determine the fractal dimension from the slope of the linear  $\ln(-\ln I(t))$  vs.  $\ln t$  plot. The results show that the equation indeed gives a straight line for a structure for which  $D/d$  is not much smaller than unity. As this ratio decreases, deviation from a straight line is obtained and an oscillating behavior appears. It is shown that, from the oscillation characteristics, the fractal dimensionality as well as other geometrical parameters characterizing the fractal structure can be determined.

#### Introduction

Fractals,<sup>2</sup> structures with dilation symmetry, have attracted a great deal of attention recently, due to their usefulness in describing disordered systems. Processes occurring in systems such as polymers<sup>3,4</sup> and proteins<sup>4,5</sup> and on surfaces<sup>6</sup> have been discussed in terms of fractals, as are the processes such as crystal growth,<sup>7</sup> dielectric breakdown,<sup>8</sup> turbulence, and chaos.<sup>9</sup> Fractals have also been used to describe the diffusion of liquids into porous media.<sup>10</sup>

Three different dimensions are at least required to define a fractal.<sup>11,12</sup> The first is the Euclidean dimension,  $d$ , in which the structure is embedded. The second is called the fractal dimension,<sup>2</sup>  $D$ . This describes the dependence of the number of the sites  $N(R)$  on the distance  $R$ , through the relation ( $N(R) = R^D$ ). The third dimension is the spectral or fracton dimension,<sup>11,12</sup>  $\tilde{d}$ , which governs the random walk and relaxation processes and determines the density of states of the structure. The spectral dimension has been previously discussed in electron-spin relaxation studies in protein<sup>4,5</sup> and triplet-triplet annihilation studies in mixed molecular crystals.<sup>13,14</sup> Recently, studies of one-step electronic energy transfer have been discussed, both theoretically<sup>1</sup> and experimentally,<sup>15</sup> in terms of fractal dimension  $D$ . Theoretically, Klafter and Blumen<sup>1</sup> (KB) extended the equation describing the time dependence of a donor intensity derived previously (Blumen et al.<sup>16</sup>) for one-step

dipolar energy transfer to fractal systems. The derivation of this equation implies continuous dilation (i.e., the open fractal structure

- (1) Klafter, J.; Blumen, A. *J. Chem. Phys.* **1984**, *80*, 875.
- (2) Mandelbrot, B. *Les Objets Fractals; Flammarion*, Paris, 1975. English Versions: *Fractals: Form, Chance and Dimension*; W. H. Freeman: San Francisco, 1977. *The Fractal Geometry of Nature*; W. H. Freeman: San Francisco, 1982.
- (3) De Gennes, P.-G. *J. Chem. Phys.* **1982**, *76*, 3316.
- (4) Allen, J. P.; Colvin, J. J.; Stimson, D. G.; Flynn, C. P.; Stapleton, H. *J. Biophys. J.* **1982**, *38*, 299.
- (5) Stapleton, H. J.; Allen, J. P.; Flynn, C. P.; Stimson, D. G.; Kurz, S. *R. Phys. Rev. Lett.* **1980**, *45*, 1456.
- (6) Avnir, D.; Farin, D. *J. Chem. Phys.* **1983**, *79*, 3536.
- (7) Witten, T. A.; Sander, L. M. *Phys. Rev. Lett.* **1981**, *47*, 1400. *Phys. Rev. B* **1983**, *27*, 5686.
- (8) (a) Pietronero, L.; Wiesmann, H. J. *J. Stat. Phys.* **1984**, *36*, 909. (b) Niemeyer, L.; Pietronero, L.; Wiesmann, H. *J. Phys. Rev. Lett.* **1984**, *52*, 1033.
- (9) (a) Ott, E.; Withers, W. D.; Yorke, J. A. *J. Stat. Phys.* **1984**, *36*, 687. (b) Procaccia, I. *J. Stat. Phys.* **1984**, *36*, 649.
- (10) (a) Wilkinson, D.; Willemsen, J. F. *J. Phys. A* **1983**, *16*, 3365. (b) Lenormand, R.; Cherbuin, C.; Zaccaro, C. C. *R. Acad. Sci. Paris, Ser. II*, **1983**, *297*, 637.
- (11) Alexander, S.; Orbach, R. *J. Phys. Lett.* **1982**, *43*, L-625.
- (12) Rammal, R.; Toulouse, G. *J. Phys. Lett.* **1983**, *44*, L-13.
- (13) (a) Klymko, P. W.; Kopelman, R. *J. Phys. Chem.* **1983**, *87*, 4565. (b) Argyrakakis, P.; Kopelman, R. *Phys. Rev. B* **1984**, *29*, 511. (c) Argyrakakis, P.; Kopelman, R. *J. Chem. Phys.* **1984**, *81*, 1015.
- (14) (a) Evesque, P. *J. Phys.* **1983**, *44*, 1217. (b) Evesque, P.; Duran, J. *J. Chem. Phys.* **1984**, *80*, 3016.

<sup>†</sup> In partial fulfillment of the Ph.D. Degree.

<sup>‡</sup> On leave from E.R.A. 133-C.N.R.S., University of Paris VI, France.